nature neuroscience

Visual field maps and stimulus selectivity in human ventral occipital cortex

Alyssa A Brewer[1], Junjie Liu[2], Alex R Wade[4] & Brian A Wandell[1,3]

Human visual cortex is organized into distinct visual field maps whose locations and properties provide important information about visual computations. There are two conflicting models of the organization and computational role of ventral occipital visual field maps. We report new functional MRI measurements that test these models. We also present the first coordinated measurements of visual field maps and stimulus responsivity to color, objects and faces in ventral occipital cortex. These measurements support a model that includes a hemifield map, hV4, adjacent to the central field representation of ventral V3. In addition, the measurements demonstrate a cluster of visual field maps in ventral occipital cortex (VO cluster) anterior to hV4. We describe the organization and stimulus responsivity of two new hemifield maps, VO-1 and VO-2, within this cluster. The maps and stimulus responsivity support a general organization of visual cortex based on clusters of maps that serve distinct computational functions.

Human visual cortex is organized into a set of distinct visual field maps; these are cortical regions in which nearby neurons analyze the properties of nearby points in the visual field. Knowledge of the properties of these visual field maps and the stimulus selectivity of the neurons within these maps is the foundation for understanding visual computations.

Although there is consensus on the properties of several human maps, including V1, V2 and V3 (refs. 1–4), there are disputes about the organization of maps in other portions of human visual cortex[5]. One of the disputed regions is the ventral occipital surface adjacent to V3 (refs. 6,7). There has been no consensus on the properties of visual field maps in this region despite several attempts to understand their organization and role in visual perception[6–15].

Here we report new measurements of eccentricity maps, angular maps and stimulus responsivity in ventral occipital cortex. These measurements discriminated between two models of the visual field maps. The data supported a model containing a hemifield map, hV4, adjacent and anterior to the ventral portion of V3. In addition, these measurements demonstrated a cluster of visual field maps containing at least two new hemifield maps, VO-1 and VO-2, anterior to hV4 on the fusiform gyrus.

To clarify the perceptual function of the neurons in these maps, we describe the first coordinated measurements of color, face and object selectivity within these visual field maps. The stimulus selectivity differed across the hV4 and VO maps. The field maps hV4, VO-1 and VO-2 responded well to color stimulus exchanges. The VO-1 and VO-2 maps responded preferentially to objects compared to faces, but the hV4 map did not. In addition, the stimulus-response patterns in hV4, VO-1 and VO-2 differed from cortex lateral to these maps.

RESULTS

Visual field map models

We compared two models of the visual field maps on the ventral surface adjacent to ventral V3 (**Figs. 1** and **2**). One, the hV4 (human V4) model, was proposed by Wade *et al.*[15] (see also Kastner *et al.*[10] and McKeefry *et al.*[8]). The second, the V8 model, was proposed by Hadjikhani *et al.*[6]. Both models agree that there are several maps representing the upper part of the visual field in a single hemisphere beginning in the calcarine sulcus and extending onto the ventral surface (**Fig. 1a**): V2-ventral (green), V3-ventral (blue) and an upper quarter-field (red) adjacent and anterior to V3v. All of these quarter-field maps share a common eccentricity profile, with the foveal representation centered slightly lateral to the occipital pole and the peripheral representation extending onto the ventral surface toward the collateral sulcus.

The models diverge in the region of cortex adjacent to these quarter-field maps in the location denoted by the dotted yellow outline. The hV4 model[15] suggests that the upper quarter-field adjacent to V3v is part of a hemifield map that extends into the dotted yellow region. The red region and outlined region together form hV4. This hemifield map has an eccentricity representation parallel to that of V1/2/3.

The V8 model proposes that the upper quarter-field adjacent to V3v, named V4v, has no corresponding lower quarter-field representation[16]. Adjacent to V4v, in the area bounded by the dotted yellow line (**Fig. 1a**), the model proposes a visual area, V8, that represents a hemifield and whose eccentricity map is rotated 90° with respect to the red region[6]. The peripheral representation of V8 abuts the horizontal meridian representation in V4v, and the foveal representation of V8 is distinct and anterior to that of V1/2/3.

[1]Neurosciences Program, [2]Applied Physics and [3]Department of Psychology, Stanford University, Stanford, California 94305, USA. [4]Smith-Kettlewell Eye Research Institute, San Francisco, California 94115, USA. Correspondence should be addressed to A.A.B. (alyssa.brewer@stanford.edu).

Published online 17 July 2005; doi:10.1038/nn1507

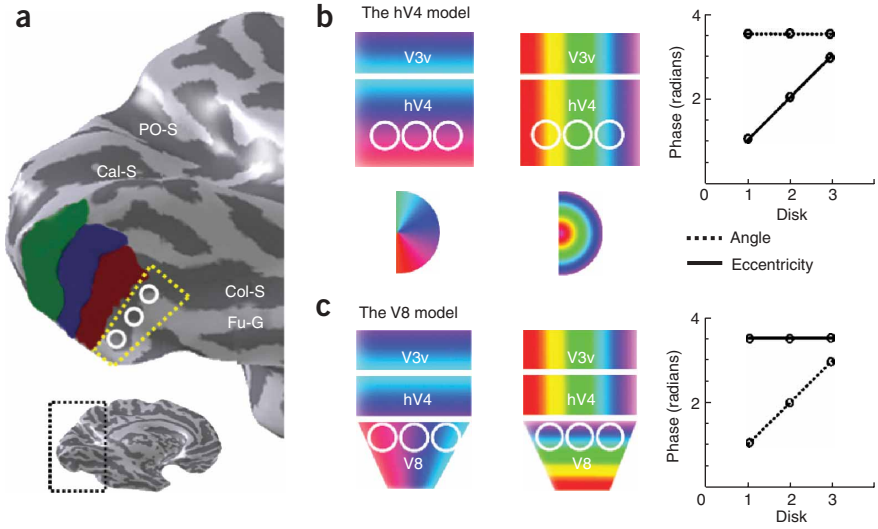

Figure 1 Ventral occipital visual field map models. (**a**) Top: locations of ventral portions of V2 (green), V3 (blue) and the undisputed quarter-field representation (red), derived from automatic atlas-fitting procedures (0–3° eccentricity[3]). The dotted yellow line and white circles denote the region of cortex in which the hV4 and V8 models diverge. Inset at lower left: region of cortex under study. PO-S: Parietal-occipital sulcus. Cal-S: Calcarine sulcus. Col-S: Collateral sulcus. Fu-G: Fusiform gyrus. (**b**) The hV4 model specifies a hemifield map adjacent and anterior to ventral V3. The colors in the cartoon maps represent the visual field position that would produce the strongest response at that cortical location (see color legends). Measurements at the positions indicated by the white circles (corresponding to the locations of the white circles in **a**) should have a constant angular representation and a varying eccentricity representation. These predictions are illustrated in the graph at the right, which shows the expected traveling wave phases in response to rotating wedge (angle) and expanding ring (eccentricity) stimuli. (**c**) The V8 model includes only a quarter-field map adjacent to the ventral portion of V3. Adjacent to this quarter-field map, the model proposes a rotated hemifield representation. The V8 model predicts that measurements at the white circle positions will have a varying angular representation and a constant eccentricity representation. These predictions are shown in the graph at the right, which can be contrasted with the predictions for the hV4 model.

The hV4 and V8 models predict different response patterns at the locations indicated by the white circles (**Fig. 1**). In the hV4 model, measurements along the white circles should represent a constant angular direction and changing eccentricity. In contrast, the V8 model predicts a constant eccentricity representation and a varying angular direction. The contrasting predictions from these two models are illustrated in the graphs in **Figure 1b**,**c**.

Testing the models

We measured the visual field representation in the disputed region using traveling wave stimuli (**Fig. 2**). These stimuli were confined within the central 3° and contained relatively high–spatial frequency patterns. The angular and eccentricity measurements are shown as pseudocolor maps in **Figure 2a**,**b**, respectively (see **Figs. 3–5** for additional examples). The white lines denote the boundary between V2v/V3v and the anterior boundary of V3v. These boundaries as well as the horizontal meridian of the undisputed quarter-field were defined by atlas-fitting procedures[3]. The white circles indicate three measurement regions comprising 3-mm-radius disks. These were positioned (i) in the disputed portion of cortex, (ii) parallel to the horizontal meridian of the undisputed upper field representation and (iii) with a spacing of approximately 1 cm center-to-center.

In all nine observers, the angular representation in these three regions was approximately constant (**Fig. 2c**). The eccentricity representation varied from fovea to periphery, paralleling that of the V2/V3 eccentricity maps. Hence, the data were consistent with the hV4 model but inconsistent with the V8 model.

In previous reports that included measurements of visual field maps in ventral occipital cortex, investigators used stimuli that spanned a much larger portion of the visual field[6,8,10,15]. Although we found that data were consistent across 20° and 3° measurements, concentrating the measurements in the central 3° provided a clearer view. This may be explained by the strong cortical magnification present in the region around hV4 and on the ventral surface in general[17]. This foveal emphasis is consistent with anatomical labeling in macaque that shows foveal receptive fields dominating the ventral pathways and dorsal pathways receiving predominantly peripheral input[18].

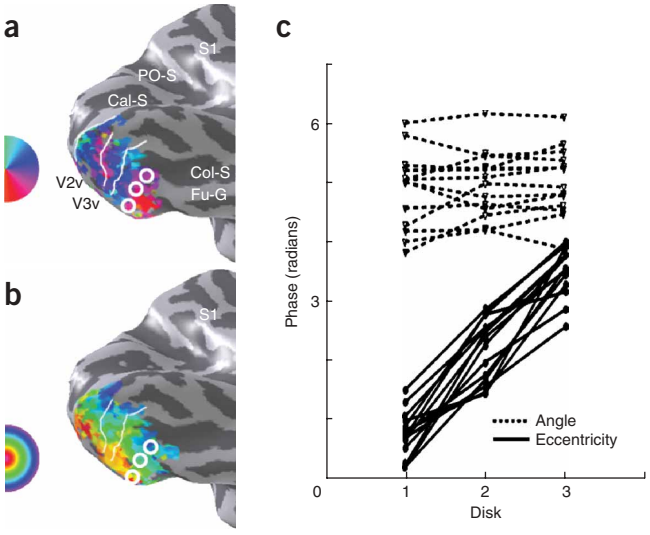

Figure 2 The data support the hV4 model. (**a**) Angular map measurements using 3° rotating wedge stimuli. The pseudocolor overlay represents the visual field position that produces the strongest response at each cortical location (see color legend). The measurements shown are restricted to lie within the boundaries of V2v, V3v and hV4, as derived from automatic atlas fitting procedures[3]. The white lines mark the boundary between V2v and V3v as well as at the anterior boundary of V3v. The white circles show the three measurement positions (3-mm-radius disks) in the disputed region. (**b**) Eccentricity map measurements using a 3° expanding ring stimulus; otherwise as in **a**. (**c**) Measurements from nine subjects showing the traveling wave phases in the 3-mm radius disks at the white circle positions (most foveal disk is #1). For clarity, the left hemisphere angular phases have been shifted up by π radians to align with the right hemisphere angular phases. Subject 1 in **a**,**b**. Coherence $\geq$ 0.30. Other details as in **Figure 1**.

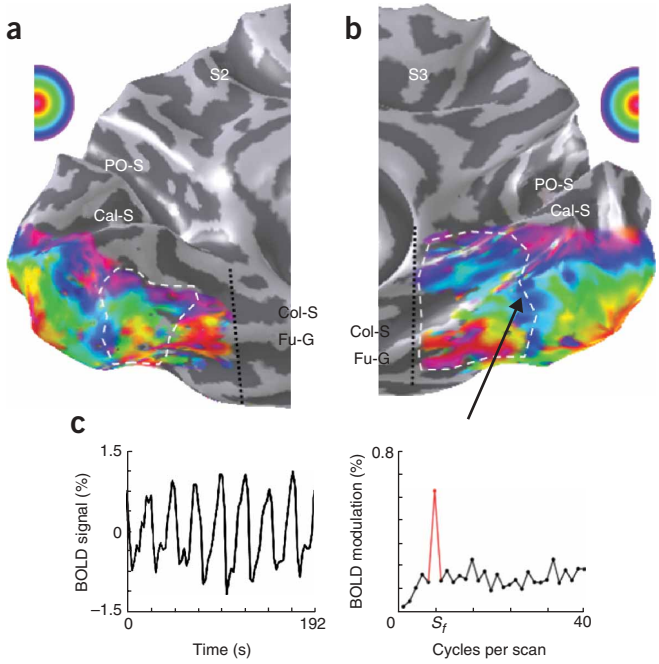

Figure 3 The VO cluster. (**a**,**b**) Eccentricity maps in ventral occipital cortex of two subjects measured using expanding ring stimuli (3°; see color legend). Two distinct foveal representations (red/yellow) are present. The posterior representation is at the confluence of the V1/V2/V3/hV4 maps. These share a common eccentricity representation that expands in a semicircle from the foveal representation. The second foveal representation is located in the fusiform gyrus and also forms a semicircular eccentricity map. The two maps meet at the blue boundary. Measurement planes were located posterior to the dotted line. For clarity, only responses near the fusiform gyrus are shown. (**c**) BOLD time series and response amplitudes in a 3-mm-radius disk located at the arrow in **b**. The normalized response amplitude at the signal frequency (S_f, red) with respect to the distribution of non-stimulus frequencies is 16.77. These stimulus-driven signals are substantially above statistical threshold. Subjects S2, S3. Coherence ≥ 0.25 (S1) or 0.20 (S6). Other details as in **Figure 2**.

HV4 and the VO cluster

In human cortex, we have proposed that visual field maps are organized into several clusters as exemplified by the V1/2/3/hV4 cluster[5]. These clusters share a common eccentricity representation and can be subdivided into multiple maps by reversals in their angular representations. In addition to the cluster near V1, there are established clusters near V3A/V3B and motion selective cortex (hMT+). We suspect that each cluster contains one or more groups of maps with similar computational functions.

Eccentricity measurements (3° expanding ring) in ventral occipital cortex revealed another cluster of maps anterior to hV4 (**Fig. 3a**,**b**). The foveal (red/yellow) representation of the V1 cluster can be seen at the occipital pole. The peripheral boundary of this cluster is also evident (cyan/blue/purple). In more anterior ventral cortex, along the fusiform gyrus and collateral sulcus, there was a distinct semicircular eccentricity map (dotted white line) on the fusiform gyrus[15]. We refer to this region as the ventral occipital (VO) cluster. We measured complete eccentricity maps in this region in all subjects. Anterior to the VO cluster, we observed additional responses to the traveling wave stimuli in many subjects, but these will not be further described here.

The blood oxygenation level-dependent (BOLD) response is strong and reliable across the boundary between hV4 and the VO cluster (**Fig. 3b**, arrow). The curve on the left (**Fig. 3c**) measures the mean of the BOLD time series $r_i(t)$. The curve on the right measures the mean of the harmonic response amplitudes across the region of interest. For a collection of time series $r_i(t)$ at voxels $i = 1,N$ in the region of interest, the mean of the harmonic amplitudes is

$$\overline{A}(f) = \frac{1}{N}\sum_{i=1,N} |F(r_i(t),f)|$$

where $F()$ is the Fourier transform operator and $|\ |$ is the amplitude operator. By computing the harmonic amplitudes at each voxel before averaging, we compared response strength independent of the phase differences between the voxels. The peak response frequency coincided with the stimulus alternation frequency (red). The response modulations were substantially higher than common statistical significance levels ($P \ll 0.001$).

New visual field maps in the VO cluster

Beyond hV4, there were at least two hemifield maps in the VO cluster, VO-1 and VO-2 (**Fig. 4**). The lower vertical meridian representation of the VO-1 map (magenta; posterior white line) abutted the peripheral representation of hV4 and extended to the peripheral representation of V3v. VO-1 and VO-2 shared an upper vertical meridian representation (cyan/blue; anterior white line).

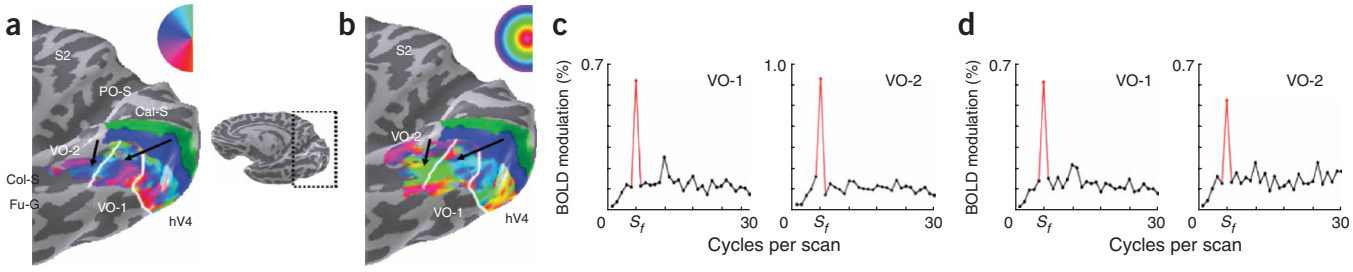

Figure 4 The definitions of VO-1 and VO-2. The solid green and blue regions in the images denote V2v and V3v (0–16°) derived from the automatic atlas-fitting procedures described in Methods[3]. The color overlays show measurements of the visual field position that most effectively stimulates each cortical location (see color legends). The inset shows the right ventral occipital region under study. (**a**) Angular map measurements using 3° rotating wedge stimuli. The white lines indicate the boundaries between hV4 and VO-1 and between VO-1 and VO-2. For clarity, data are restricted to hV4, VO-1 and VO-2 maps, as defined by the atlas fitting procedures. (**b**) Eccentricity map measurements using a 3° expanding ring stimulus; otherwise as in **a**. (**c**,**d**) The response amplitudes as a function of temporal frequency measured in two 3-mm-radius disks located in VO-1 and VO-2 (arrows). The responses for both angular (**c**) and eccentricity (**d**) data are significantly greater at the stimulus repetition frequency (6 cycles/scan, shown in red) than other temporal frequencies. Normalized response amplitude at the signal frequency (S_f, red) with respect to the distribution of non-stimulus frequencies are 12.14, 12.37 (VO-1, wedge and ring) and 17.55, 8.54 (VO-2, wedge and ring). Subject S2. Coherence ≥ 0.25. Other details as in **Figure 2**.

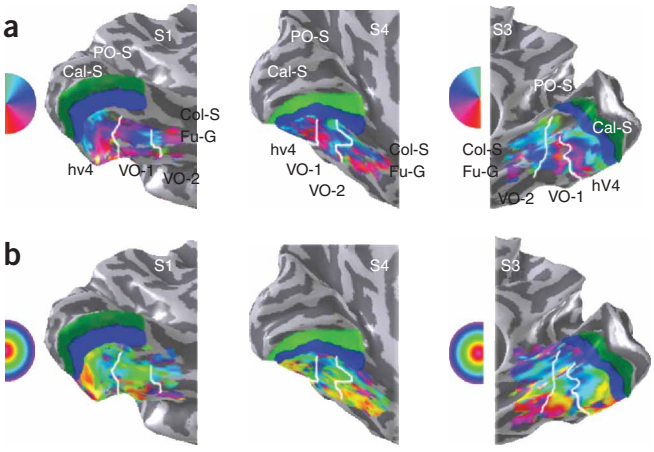

Figure 5 Additional examples of hV4, VO-1 and VO-2. Solid green and blue regions: ventral V2 and V3 (0–16°), respectively, derived from the automatic atlas-fitting procedures[3]. The color overlays show measurements of the visual field position that most effectively stimulates each cortical location (see color legends). Panels **a** and **b** show angular and eccentricity maps, respectively. Subjects S1 (left hemisphere), S3 (right hemisphere), S4 (left hemisphere). Coherence $\geq$ 0.15. Other details as in **Figure 4a**,**b**.

The VO-1 and VO-2 eccentricity maps began in the large distinct foveal representation used to define the VO cluster. Much like the V3A/V3B maps, the eccentricity representation formed a semicircular pattern. The eccentricity map became increasingly peripheral as it extended medially across the collateral sulcus and approached the peripheral representation of V3v.

The arrows in **Figure 4a** indicate the location of two regions of interest (3-mm-radius disks). The harmonic amplitudes of BOLD responses in these two regions are shown in the graphs at the bottom (**Fig. 4c**,**d**). Again, the response modulations were substantially higher than common statistical significance levels ($P \ll 0.001$).

The same basic pattern of visual field maps is shown in three additional subjects (**Fig. 5**). An angular map representing the complete VO-1 and VO-2 hemifield was present in all subjects measured ($n = 9$), although the precise orientation with respect to the sulcal and gyral patterns varied across subjects. Because the relatively anterior location of VO-2 within visual cortex was at the limit of the volume that could be imaged by our posterior surface coil, the signal coherence within VO-2 was lower than the coherence in more posterior regions in some subjects.

The maps in this region occupied small amounts of cortical surface area, so that with current fMRI spatial resolution (2.5 mm), the maps depend on measurements in only a few dozen spatial samples, and these samples might not be completely independent. Because of the limited spatial resolution of the measurements, it is important to make additional measurements of stimulus selectivity to clarify the presence (or absence) of a visual field map boundary. In the next section, we describe coordinated measurements of color, object and face responsivity within these maps and adjacent regions to further clarify the properties and functional significance of these maps.

Stimulus selectivity near hV4, VO-1 and VO-2

Cortical computations in ventral occipital cortex are important for many types of visual recognition processes. Lesions in this region can cause selective loss of color, face or object perception[19–23]. There are significant fMRI responses in these regions as subjects engage in a wide range of tasks involving color, faces, or objects[9,24–27]. Using the same set of subjects as in the visual field mapping experiments, we measured stimulus-exchange responses in this ventral region in order to clarify the relationship between the visual field maps in this region and the responses to these stimuli.

We identified nine regions of interest (ROIs) for measurements spanning hV4 (red), VO-1 (yellow), VO-2 (magenta) and nearby lateral cortex (white circles in **Fig. 6**). Each ROI within the maps was centered over a 3-mm-radius disk as measured on the cortical surface; the lateral ROIs had a 6 mm radius. The hV4 (circles labeled 1 and 2), VO-1 (circles 3,4), and VO-2 (circles 5,6) ROIs were placed approximately on the horizontal meridian in foveal and peripheral representations.

We measured the responses in these nine ROIs during color-luminance exchange experiments (**Fig. 7a**) and object-face exchange experiments (**Fig. 7b**). In these exchange experiments, we expected the responses across voxels in an ROI to occur in a common temporal phase. Hence, we measured the response by first computing the average time series of all the voxels in the region of interest and then calculating the amplitude spectrum of this average. That is, for a response time series $r_i(t)$ at voxels $i = 1,N$ in the region of interest, we calculated the amplitude spectrum as

$$A(f) = \left| F\left(\frac{1}{N} \sum_{i=1,N} r_i(t), f \right) \right|$$

We summarized the response during the exchange experiment by computing the normalized response amplitude. This quantity was computed from the BOLD response amplitude at the stimulus exchange frequency, $A(f_S)$, the mean amplitude at noise frequencies,

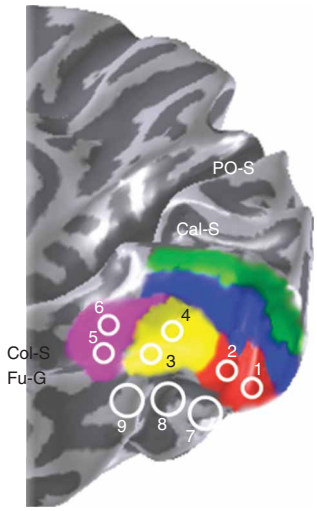

Figure 6 Stimulus selectivity measurement locations. The solid colored regions denote ventral visual maps fit by the automatic atlas fitting procedures[3]: V2 (green, 0–16°), V3 (blue, 0–16°), hV4 (red), VO-1 (yellow) and VO-2 (magenta). The white circles show the nine measurement locations. The regions in hV4, VO-1 and VO-2 are 3-mm-radius disks; those lateral to these maps are 6-mm radius. Each map contains a relatively central and peripheral measurement region near the horizontal meridian representation. PO-S: parietal-occipital sulcus. Cal-S: calcarine sulcus. Col-S: collateral sulcus. Fu-G: fusiform gyrus.

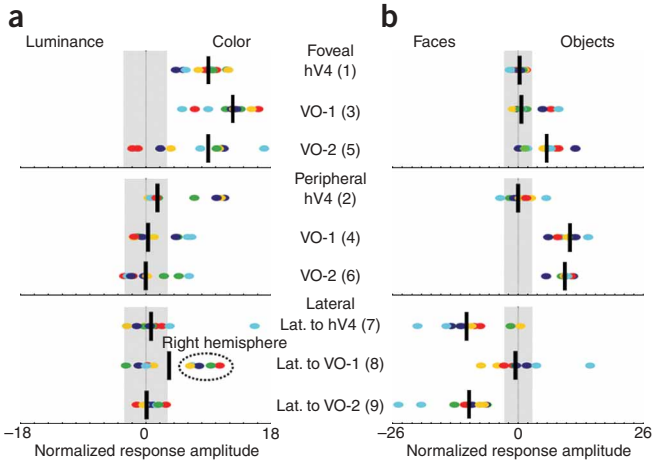

Figure 7 Stimulus selectivity measurements. The normalized response amplitudes in nine ROIs during the color-luminance (**a**) and object-face (**b**) experiments are shown. The top and middle panels show the responses in the central (1,3,5) and peripheral (2,4,6) ROIs (numbers in parentheses indicate ROI numbers; see **Fig. 6**). The bottom panel shows the responses in the three regions lateral to the maps (7,8,9). The circles represent the normalized responses for individual subjects ($n = 5$, two hemispheres per subject) and are colored by subject. The dark vertical bars represent the median response. The shaded regions represent a significance level $P > 0.001$ (uncorrected). The dotted oval indicates measurements from the right hemisphere. Subjects S1, S2, S4, S5, S6.

$\langle f_N \rangle$ (frequencies other than f_S and $2f_S$) and the s.d. of the amplitude at the noise frequencies, $\sigma_{\langle f_N \rangle}$.

$$\overline{R} = \left| \frac{A(f_s) - \frac{1}{N} \sum_{\langle f_N \rangle} A(f_N)}{\sigma_{\langle f_N \rangle}} \right|$$

We assigned the normalized response a positive or negative value to indicate which of the stimulus phases aligned with the response phase (for example, positive BOLD responses in synchrony with object or face presentations).

The normalized response amplitudes in each of the nine ROIs during the color-luminance exchange experiments are shown in **Figure 7a**. There was a significant response in synchrony with the color stimulus in all three maps; the response amplitude was significantly greater in the central than peripheral portions of the maps.

We were surprised to find that there was a significant right/left hemisphere difference in the responses lateral to VO-1 (ROI 8). There were powerful color responses in the right, but not left, hemisphere of all five subjects. (All five subjects were right-handed.) No other differences in lateralization were observed.

The normalized response amplitudes in each of the nine ROIs during the object-face exchange experiments are shown in **Figure 7b**. There was no preferential response in either the central or peripheral ROIs of hV4. In additional measurements, we found that the upper and lower field representations of hV4 were consistent in both the color-luminance and object-face experiments, supporting the grouping of the upper and lower quarter-field representations within hV4 into a single hemifield representation.

In both VO-1 and VO-2, there was a stronger preference for objects, particularly in the peripheral portions of these maps. Responses in phase with the face presentations were observed in the regions lateral to hV4 and VO-2. These ROIs were near the Talairach coordinates of two commonly cited face-responsive regions: the fusiform face area[27,28] and the occipital face area[24]. The Talairach coordinates for the parahippocampal place area were anterior and slightly lateral to VO-2 (ref. 29). An example of the spatial distribution of color, face and object responses in relation to visual field maps is shown for one subject in **Supplementary Figure 1**.

In summary, the stimulus selectivity properties of hV4, the VO cluster maps, and the lateral regions all differed from one another.

DISCUSSION

To investigate the visual computations in ventral occipital cortex, we made measurements of visual field maps coordinated with selectivity for color, faces and objects.

Visual field maps

Figure 8a summarizes the ventral maps beyond V1. The ventral portions (0–16°) of the V2 and V3 maps both represented the upper visual field. The hV4, VO-1 and VO-2 maps spanned a hemifield. The relatively central representations of the V2, V3 and hV4 maps were confluent with the V1 central representation. The central representations for V1, V2 and V3 extended onto the lateral surface (data not shown), but the hV4 central representation remained ventral. The VO-1 and VO-2 maps shared a central representation that was separated from the V1/2/3/hV4 fovea and located primarily along the fusiform gyrus.

When measured using a 3° radius stimulus, the hV4 map covered a surface area of about 500–750 mm^2 (**Fig. 8b**). The VO-1 and VO-2 maps were both slightly smaller than hV4 (400–700 mm^2). Like V1, the surface area of each of these maps varied across subjects[3]. Individual map sizes for V1, hV4, VO-1 and VO-2 are described in **Supplementary Table 1**. When measuring V1 with the same 3° stimulus, the

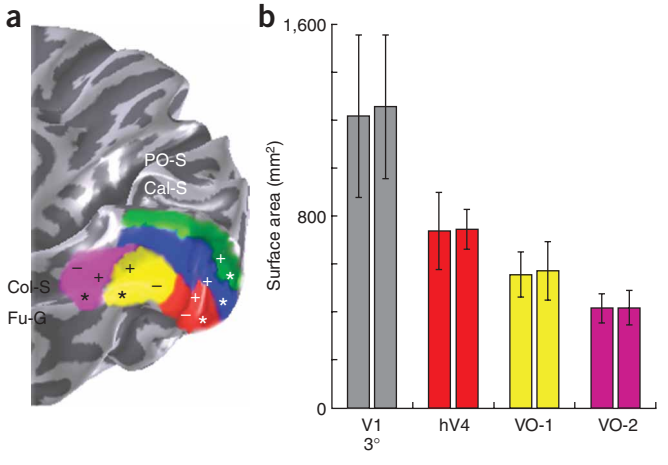

Figure 8 Summary of hV4, VO-1 and VO-2 field map properties. (**a**) The positions of the ventral-occipital visual field maps V2v (green, 0–16°), V3v (blue, 0–16°), hV4 (red), VO-1 (yellow) and VO-2 (magenta) are shown. The + and – indicate upper and lower visual field representations, respectively. The asterisk indicates the most central visual field representation within each map. PO-S: parietal-occipital sulcus. Cal-S: calcarine sulcus. Col-S: collateral sulcus. Fu-G: fusiform gyrus. (**b**) The surface area of each map was defined by a 3° expanding ring stimulus and measured along the cortical manifold. The left and right hemispheres correspond to the left and right bars. Error bars: ± 1 s.d.

cortical surface area spanned approximately 600–1600 mm^2. When measured using a 16° stimulus, the responding surface area of V1 expanded considerably along the calcarine sulcus, but the hV4, VO-1 and VO-2 maps expanded very little or not at all. These ventral maps appeared to respond more powerfully to central visual stimuli throughout their extent, consistent with the strong cortical magnification described in human and macaque ventral cortex[17,18].

These data are the first report in the literature on human hemifield maps in the positions occupied by VO-1 and VO-2. The VO cluster occupies the same position as the object-responsive region that Halgren *et al.* refer to as posterior collateral[30] and the building-responsive region that Malach *et al.* refer to as collateral sulcus (see Figure 3 in ref. 11). Halgren *et al.* describe this region as non-retinotopic cortex; Malach *et al.* describe it as having only a peripheral eccentricity bias and no angular representation. In contrast to both studies, we found two visual field maps (VO-1, VO-2) in this region with detailed eccentricity and angular maps that were primarily central.

The visual field maps measured here can be compared with several other reports in the literature. We have already described the differences between our hV4 measurements and the V8 model[6]. Our hV4 measurements are consistent with those of Kastner *et al.*[10], who describe a hemifield adjacent to V3v and find no evidence for the V8 visual field map. Tootell *et al.*[16] (subsequent to Halgren *et al.*) have reported data consistent with a full visual hemifield map adjacent to V3v (see Figures 5 in refs. 16,31). The organization of the ventral maps was secondary to those papers, and the authors did not discuss this aspect of their measurements. McKeefry and Zeki[8] have also demonstrated a hemifield map in the ventral region. In subsequent measurements, this group identified a V4 complex (V4; V4α) that overlaps with hV4 and the VO cluster[9]. They did not measure visual field maps near this region, such as V2 and V3, leaving open how their activations are positioned with respect to those maps.

The region anterior to hV4 on the fusiform gyrus, which overlaps with the VO cluster, has also been discussed by Kastner *et al.*[10,32]. They call this region TEO based on its position and a guess about homology with macaque. While they show that this region responds to stimuli across the contralateral hemifield, they find no separation between the upper and lower visual field representation and do not measure eccentricity maps.

We have considered the relationship between the model we present here and the V8 model proposed by Hadjikhani *et al.*[6]. One way to coordinate these models is to suppose that Hadjikhani *et al.* missed the second quarter-field in hV4, but that VO-1 is the visual field map they identified as V8. We call this a quarter-field-insertion model. According to this model the VO-1 visual field map should have (i) a peripheral representation that abuts the hV4 lower vertical meridian and (ii) an angular representation that runs parallel to the hV4 eccentricity map (**Fig. 1**). It would not be expected that VO-1 would reach V3v. In contrast, the VO-1 map we measured was located near the peripheral representation of hV4, nestled between that map and the peripheral representation of V3. Hence, the quarter-field-insertion model does not fit the VO-1 data, and VO-1 cannot be the same as V8. Further, the anatomical location and object-selectivity of VO-1 correlates with the object-responsive region named posterior collateral, not V8, in data from the same group[30].

A variant of the quarter-field-insertion model would allow that VO-1 is new and differs from V8, but that V8 still exists at the location abutting the lower vertical meridian representation of hV4 (see ROIs 7–8 in **Fig. 6**). We have not been able to find evidence for a V8 visual field map in this location, although we acknowledge that such evidence might be found with other stimuli or experimental designs. We do see a strong color response in position 8, lateral to VO-1, but only in the right hemisphere.

The Talairach coordinates of the hV4, VO-1 and VO-2 field maps are described in **Supplementary Table 2**. The basic arrangement of visual field maps was consistent, but across individuals there was variability on the order of 1 cm in the Talairach coordinates of these maps. Given that the maps themselves are on the order of 2–3 cm, such variability suggests that averaging across subjects would obscure the presence of these maps.

Although many aspects of human visual field maps in early visual areas parallel those in macaque, we found significant differences beyond V3v/VP. The visual field map adjacent to V3v represents a hemifield confined entirely to the ventral surface in human (hV4), while the same region in macaque (V4) continues to follow the V1/2/3 pattern of splitting into dorsal and ventral quarter-fields. The human hV4 map may be homologous to macaque V4 despite the ventral placement of the full hemifield, or hV4 may not have an exact counterpart in macaque[15,33].

The VO maps occupied a position with respect to V3v and hV4 that was similar to the position of macaque VTF[30,34,35]. Although both macaque VTF and the human VO maps are responsive to more complex visual stimuli like objects, presently there is no strong evidence linking these regions[36].

Stimulus selectivity

The patterns of stimulus selectivity in the hV4 and the VO maps differed, and these patterns both differed from those in the regions lateral to these maps. The central hV4 ROI responded powerfully to color, and no part of the map responded preferentially to faces or objects. The VO cluster maps responded strongly to color in the central portion of the map and preferentially to objects compared with faces, particularly in the peripheral representation. In contrast, cortex slightly lateral to these maps responded preferentially to faces compared to objects. This differential stimulus selectivity across this ventral region supports our definitions of the hV4, VO-1 and VO-2 visual field maps.

There is consensus that ventral occipital cortex is essential for normal color perception. However, there is a dispute about the localization of color processing with respect to individual maps[6–9,37,38]. McKeefry and Zeki[8] describe a V4 complex as the essential region for color perception, while Hadjikhani *et al.*[6] propose that V8 is the essential map. Both groups identify essential color signals by measuring the response while alternating two stimuli. However, these stimulus pairs are not comparable. McKeefry and Zeki use a spatial pattern comprised of a set of rectangles whose average luminance contrast is constant between blocks and whose chromatic contrast is modulated. Hadjikhani *et al.* use harmonic patterns that alternate between a 95% contrast monochrome pattern and an isoluminant chromatic pattern (unspecified contrast level); in these experiments neither luminance nor chrominance are held constant. These two types of stimulus alternations should not produce identical cortical responses. For example, the McKeefry and Zeki stimulus would produce no modulation in regions that respond only to luminance, whereas the Hadjikhani *et al.* stimulus would.

The color-luminance exchange measurements performed here used the same approach as McKeefry and Zeki[8] and produce responses in hV4, VO-1 and VO-2. In separate experiments, we have also used the Hadjikhani *et al.*[6] design, and we found that the spatial distribution of responses in phase with the color stimulus was nearly identical in both experiments. Hence, we believe that the Hadjikhani *et al.* color responses are in the same cortical locations as described by McKeefry and Zeki[8] and colleagues[9,37,39].

Neither group comments on the right lateralization of the color responses, which we observed using both types of color-luminance exchange methods. In addition, our color responses were not confined to a single visual field map, in contrast to reports from Hadjikhani *et al.*[6]. Before drawing strong conclusions about the functional role of these responses in color perception, a variety of additional factors, such as the spatial inhomogeneity of the retinal encoding of signals and better stimulus control, must be accounted for (for example, see refs. 4,15,40).

Visual clusters

In human, we find several distinct eccentricity maps that include one or more angular maps (**Figs. 3–5**). We have named such regions visual field map clusters[5]. The V1/V2/V3/hV4 maps form one cluster; the V3A/V3B maps form another; the maps near hMT+ form another cluster; and we propose that VO-1 and VO-2 are part of a VO cluster.

We suspect that maps within each cluster share common computational resources, such as short-term information storage or timing circuitry[41]. It may also be that perceptual specializations are organized around these clusters rather than within single visual field maps, as is seen in the common motion selectivity in the hMT+ cluster. The data presented here show common object and color selectivity across the VO cluster.

The visual cluster model differs from the model of human visual cortex developed by Levy *et al.*[12–14,42]. According to that model, visual cortex begins with precise visual field maps in V1, V2, and V3. Anterior to these regions, however, the maps degrade, so that "orderly representations of the visual field meridians are absent" (ref. 12, p. 533). The contiguous eccentricity map present in the early visual areas degrades to become simply a bias toward central and peripheral responses[14]. These eccentricity biases are posited as the driving force for organization in higher order visual cortex. The eccentricity bias theory does not allow for the detailed eccentricity and angular maps as seen in VO-1 and VO-2.

We disagree with their model because (i) no computational principle has been identified to suggest why neurons would be arranged with orderly eccentricity responses, but no angular maps, and (ii) we observe organized eccentricity and angular maps in ventral cortex (see ref. 5 for an extended critique). Hence, we propose exploring the alternative hypothesis that clusters of maps, each devoted to a different computational function, are a basis for the organization of human visual cortex.

METHODS

Subjects. Nine subjects participated in this study (visual field mapping: S1–S9; stimulus selectivity: S1, S2, S4–S6). All subjects had normal color vision and a corrected acuity of 20/20 or better. Informed written consent was obtained from all subjects.

Visual display. Stimuli were presented on an LCD (NEC 2080UX; spatial resolution 800 × 600, refresh rate 60 Hz). The display was inside an electrically shielded box with conductive glass on the front side. The intensity and spectral characteristics of the display were calibrated (PhotoResearch PR-650). The display primary intensities were controlled using a 10-bit digital-to-analog card (ATI Radeon). Cone excitations were estimated using conventional methods[43,44].

Stimuli were presented in one of two display configurations. (i) The visual field mapping studies were performed with the LCD positioned at the rear of the magnet bore, behind the subject's head. The viewing distance was 2.8 m. Subjects viewed the LCD through an angled front surface mirror placed close to the eyes. The mirror was included in the optical path during the display calibration procedure. The maximum stimulus radius subtended 3° of visual angle. (ii) The stimulus selectivity studies (faces, objects, and color) were performed with the display at the foot of the patient table. In this configuration subjects viewed the screen through binoculars as well as the mirror. The binoculars were adjusted to ensure that the stimulus was centered in the visual field and no vignetting occurred. The monitor was 4.3 m from the subject, so the approximately eightfold magnification of the binoculars yielded an effective viewing distance of 0.54 m. In this configuration, the maximum stimulus radius subtended 16° of visual angle.

FMRI data acquisition. FMRI measurements were performed on a 3-T General Electric scanner with a custom-designed surface coil (Nova Medical) for anatomical, visual field mapping and color scans or with a custom-built volume head coil for the object-face scans. Subjects were supine in the scanner bore, with the coil placed near visual cortex. Head movements were minimized by padding and tape. Functional MR data were acquired with a spiral pulse sequence[45,46] with 21–30 slices oriented coronally, axially or perpendicularly to the calcarine sulcus. Slice orientation had no significant effect on results. The effective inter-frame sampling interval of BOLD signals was 2.4 s (field mapping) or 3 s (stimulus selectivity), and the voxel size of functional data was 2.5 × 2.5 × 3 mm.

A set of two-dimensional fast SPGR anatomy images was acquired before the series of functional scans. These T1-weighted slices were physically in register with the functional slices and were used to align the functional data with the high-resolution anatomy data via a semi-automated three-dimensional (3D) coregistration algorithm[47].

Data analysis. We analyzed fMRI data using custom software (http://white.stanford.edu/software/). Data in each fMRI session were analyzed voxel-by-voxel with no spatial smoothing. The acquired BOLD signal from each voxel was divided by its mean to derive a time series of percent modulation. Baseline drifts were removed from the time series by high-pass temporal filtering. Head movements across scans were examined by comparing the mean value maps of the BOLD signals; most scans had minimal head motion (less than one voxel). Motion artifacts within each scan were also monitored. Fewer than 10% of the scans had significant motion artifacts; these scans were discarded. No motion-correction algorithm was applied.

Anatomical pre-processing. Anatomical images were acquired on a GE 1.5-T Signa LX scanner using a 3D SPGR pulse sequence (1 echo, minimum TE, 15° flip angle, 2 excitations). Sagittal slices were acquired with an inplane voxel size 0.94 × 0.94 mm and 1.2 mm slice thickness. We acquired 1–3 whole brain T1-weighted anatomical data sets for each subject. These images were averaged and re-sampled into a 1 × 1 × 1 mm resolution three-dimensional anatomical volume that was corrected for inhomogeneity and linearly transformed (with no rescaling or distortion) to align with the Talairach reference brain. These operations were performed using tools from the FMRIB software library (http://www.fmrib.ox.ac.uk/fsl/).

Gray and white matter were segmented from the anatomical volume using custom software and then hand-edited to minimize segmentation errors[48]. Data analysis was restricted to the gray matter. The surface at the white/gray boundary was rendered as a smoothed three-dimensional surface using VTK software (http://www.vtk.org/). Analyses were also performed on a flattened two-dimensional map of the cortical surface[40].

Visual field mapping methods. We measured visual field maps using expanding rings and rotating wedges. Stimuli were high contrast dartboard patterns[4,49]. The patterns were 5 cycles per degree (3° stimuli) or 1 cycle per degree (16° stimuli) in the radial direction, 12 cycles per 2π radians in the angular direction, and reversed contrast at a temporal frequency of 2 Hz. The expanding ring contrast pattern covered 25% of the 0–3° or 0–16° eccentricity range and changed position every 2.4 s. The wedge angle was 45° and stepped 36° clockwise every 2.4 s. For both stimuli, a full display cycle comprised 24 s, and the data include at least 25 cycles from repeated scans of each type of stimulus. Subjects maintained fixation on a central cross throughout all scans.

Atlas fitting procedures. We used an automated atlas fitting procedure to identify visual areas[3]. The algorithm simultaneously fits both angle and eccentricity maps. With this approach, we obtain objective estimates of the boundaries of hemifield and quarter-field visual angle representations.

Stimulus selectivity methods: color. Color responses were measured using a block design in which 12-s blocks of achromatic stimuli alternated with 12-s

blocks of chromatic stimuli (24-s period). Subjects viewed a series of patterns comprised of an array of 8 × 8 rectangular patches spanning 24° of visual angle. During each 12-s block a new pattern was presented every 2 s.

Stimulus color was specified in terms of relative L, M and S-cone excitations. In the first 12-s block the patterns had only achromatic (luminance scaling) contrast. In this block, (L + M)- and S-cone contrasts were set equal, and (L – M)-cone contrast was zero. The (L + M)-and S-cone contrasts were selected randomly and uniformly from a range of ±17%. In the second 12-s block, the (L + M)- and S-cone contrasts were equal and selected the same way as in the first block. The (L – M)-cone contrast was selected randomly and uniformly from a contrast range of ±6%. The two contrast ranges (17% for (L + M)-cone and S-cone compared with 6% for (L – M) chromatic) were chosen to approximately equate for V1 responses[50].

To control attention, subjects were required to detect the orientation of a superimposed 'C' shape. The shape was created by adding a small amount of L + M signal to seven of the rectangles. The additional mean signal was very slight and was adjusted so that subjects scored about 80% correctly in identifying the orientation of the target.

Stimulus selectivity methods: faces and objects We measured fMRI responses to stimuli by alternating between blocks containing images of faces and blocks containing a variety of objects. A new grayscale picture within one category (for example, face) was presented every 2 s during a 36-s block. All photographs were scaled to subtend 12 × 12° of visual angle, matched in mean luminance, and centered in the visual field. These stimuli were similar to those used by Kanwisher and colleagues in studies examining face and object representations[26,27].

Throughout each scan, subjects maintained fixation on a 0.2° cross that was centered in the field of view. To control for attention, the subjects were asked to perform a one-back matching task in which they compared the present picture to the stimulus presented two frames prior. One or two pictures per block were repeated.

Note: Supplementary information is available on the Nature Neuroscience website.

ACKNOWLEDGMENTS

Supported by National Eye Institute RO1 EY03164 and National Institute of Neurological Disorders and Stroke 5 F30 NS44759.

COMPETING INTERESTS STATEMENT

The authors declare that they have no competing financial interests.

Received 18 May; accepted 27 June 2005
Published online at http://www.nature.com/natureneuroscience/

1. Sereno, M.I., McDonald, C.T. & Allman, J.M. Analysis of retinotopic maps in extrastriate cortex. *Cereb. Cortex* **4**, 601–620 (1994).
2. DeYoe, E.A. *et al.* Mapping striate and extrastriate visual areas in human cerebral cortex. *Proc. Natl. Acad. Sci. USA* **93**, 2382–2386 (1996).
3. Dougherty, R.F. *et al.* Visual field representations and locations of visual areas V1/2/3 in human visual cortex. *J. Vis.* **3**, 586–598 (2003).
4. Engel, S.A., Glover, G.H. & Wandell, B.A. Retinotopic organization in human visual cortex and the spatial precision of functional MRI. *Cereb. Cortex* **7**, 181–192 (1997).
5. Wandell, B.A., Brewer, A.A. & Dougherty, R.F. Visual field map clusters in human cortex. *Phil. Trans. R. Soc. Lond. B* **360**, 693–707 (2005).
6. Hadjikhani, N., Liu, A.K., Dale, A.M., Cavanagh, P. & Tootell, R.B.H. Retinotopy and color sensitivity in human visual cortical area V8. *Nat. Neurosci.* **1**, 235–241 (1998).
7. Zeki, S., McKeefry, D.J., Bartels, A. & Frackowiak, R.S. Has a new color area been discovered? *Nat. Neurosci.* **1**, 335–336 (1998).
8. McKeefry, D.J. & Zeki, S. The position and topography of the human colour centre as revealed by functional magnetic resonance imaging. *Brain* **120**, 2229–2242 (1997).
9. Bartels, A. & Zeki, S. The architecture of the colour centre in the human visual brain: new results and a review. *Eur. J. Neurosci.* **12**, 172–193 (2000).
10. Kastner, S. *et al.* Modulation of sensory suppression: implications for receptive field sizes in the human visual cortex. *J. Neurophysiol.* **86**, 1398–1411 (2001).
11. Malach, R., Levy, I. & Hasson, U. The topography of high-order human object areas. *Trends Cogn. Sci.* **6**, 176–184 (2002).
12. Levy, I., Hasson, U., Avidan, G., Hendler, T. & Malach, R. Center-periphery organization of human object areas. *Nat. Neurosci.* **4**, 533–539 (2001).
13. Hasson, U., Levy, I., Behrmann, M., Hendler, T. & Malach, R. Eccentricity bias as an organizing principle for human high-order object areas. *Neuron* **34**, 479–490 (2002).
14. Hasson, U., Harel, M., Levy, I. & Malach, R. Large-scale mirror-symmetry organization of human occipito-temporal object areas. *Neuron* **37**, 1027–1041 (2003).
15. Wade, A.R., Brewer, A.A., Rieger, J.W. & Wandell, B.A. Functional measurements of human ventral occipital cortex: retinotopy and colour. *Phil. Trans. R. Soc. Lond. B* **357**, 963–973 (2002).
16. Tootell, R.B. & Hadjikhani, N. Where is 'dorsal V4' in human visual cortex? Retinotopic, topographic and functional evidence. *Cereb. Cortex* **11**, 298–311 (2001).
17. Ejima, Y. *et al.* Interindividual and interspecies variations of the extrastriate visual cortex. *Neuroreport* **14**, 1579–1583 (2003).
18. Baizer, J.S., Ungerleider, L.G. & Desimone, R. Organization of visual inputs to the inferior temporal and posterior parietal cortex in macaques. *J. Neurosci.* **11**, 168–190 (1991).
19. Meadows, J. Disturbed perception of colours associated with localized cerebral lesions. *Brain* **97**, 615–632 (1974).
20. Meadows, J.C. The anatomical basis of prosopagnosia. *J. Neurol. Neurosurg. Psychiatry* **37**, 489–501 (1974).
21. Damasio, A., Yamada, T., Damasio, H., Corbett, J. & McKee, J. Central achromatopsia: behavioral, anatomic, and physiologic aspects. *Neurology* **30**, 1064–1071 (1980).
22. Damasio, A.R., Damasio, H. & Van Hoesen, G.W. Prosopagnosia: anatomic basis and behavioral mechanisms. *Neurology* **32**, 331–341 (1982).
23. James, T.W., Culham, J., Humphrey, G.K., Milner, A.D. & Goodale, M.A. Ventral occipital lesions impair object recognition but not object-directed grasping: an fMRI study. *Brain* **126**, 2463–2475 (2003).
24. Gauthier, I., Skudlarski, P., Gore, J.C. & Anderson, A.W. Expertise for cars and birds recruits brain areas involved in face recognition. *Nat. Neurosci.* **3**, 191–197 (2000).
25. Ishai, A., Ungerleider, L.G., Martin, A. & Haxby, J.V. The representation of objects in the human occipital and temporal cortex. *J. Cogn. Neurosci.* **12**, 35–51 (2000).
26. Grill-Spector, K., Knouf, N. & Kanwisher, N. The fusiform face area subserves face perception, not generic within-category identification. *Nat. Neurosci.* **7**, 555–562 (2004).
27. Kanwisher, N., McDermott, J. & Chun, M.M. The fusiform face area: a module in human extrastriate cortex specialized for face perception. *J. Neurosci.* **17**, 4302–4311 (1997).
28. Grill-Spector, K. *et al.* Differential processing of objects under various viewing conditions in the human lateral occipital complex. *Neuron* **24**, 187–203 (1999).
29. Epstein, R. & Kanwisher, N. A cortical representation of the local visual environment. *Nature* **392**, 598–601 (1998).
30. Halgren, E. *et al.* Location of human face-selective cortex with respect to retinotopic areas. *Hum. Brain Mapp.* **7**, 29–37 (1999).
31. Sasaki, Y. *et al.* Local and global attention are mapped retinotopically in human occipital cortex. *Proc. Natl. Acad. Sci. USA* **98**, 2077–2082 (2001).
32. Kastner, S., De Weerd, P., Desimone, R. & Ungerleider, L.G. Mechanisms of directed attention in the human extrastriate cortex as revealed by functional MRI. *Science* **282**, 108–111 (1998).
33. Gattass, R., Sousa, A.P. & Gross, C.G. Visuotopic organization and extent of V3 and V4 of the macaque. *J. Neurosci.* **8**, 1831–1845 (1988).
34. Boussaoud, D., Desimone, R. & Ungerleider, L.G. Visual topography of area TEO in the macaque. *J. Comp. Neurol.* **306**, 554–575 (1991).
35. Van Essen, D.C. Organization of visual areas in macaque and human cerebral cortex. in *The Visual Neurosciences* (eds. Chalupa, L.M. & Werner, J.S.) 507–521 (Bradford Books, Boston, 2003).
36. Rosa, M.G. & Tweedale, R. Brain maps, great and small: lessons from comparative studies of primate visual cortical organization. *Phil. Trans. R. Soc. Lond. B* **360**, 665–691 (2005).
37. Zeki, S. & Bartels, A. The clinical and functional measurement of cortical (in)activity in the visual brain, with special reference to the two subdivisions (V4 and V4 alpha) of the human colour centre. *Phil. Trans. R. Soc. Lond. B* **354**, 1371–1382 (1999).
38. Beauchamp, M.S., Haxby, J.V., Jennings, J.E. & DeYoe, E.A. An fMRI version of the Farnsworth-Munsell 100-Hue test reveals multiple color-selective areas in human ventral occipitotemporal cortex. *Cereb. Cortex* **9**, 257–263 (1999).
39. Zeki, S. *et al.* A direct demonstration of functional specialization in human visual cortex. *J. Neurosci.* **11**, 641–649 (1991).
40. Wandell, B.A., Chial, S. & Backus, B. Visualization and measurement of the cortical surface. *J. Cogn. Neurosci.* **12**, 739–752 (2000).
41. Wandell, B.A., El Gamal, A. & Girod, B. Common principles of image acquisition systems and biological vision. *Proc. IEEE* **90**, 5–17 (2002).
42. Levy, I., Hasson, U., Harel, M. & Malach, R. Functional analysis of the periphery effect in human building related areas. *Hum. Brain Mapp.* **22**, 15–26 (2004).
43. Brainard, D.H. & Colorimetry in *Handbook of the Optical Society* Vol. 1. (ed. Bass, M.) 26.1–26.54 (McGraw-Hill, New York, 1995).
44. Wandell, B.A. *Foundations of Vision* (Sinauer, Sunderland, MA,, 1995).
45. Glover, G.H. & Lai, S. Self-navigated spiral fMRI: interleaved versus single-shot. *Magn. Reson. Med.* **39**, 361–368 (1998).
46. Glover, G.H. Simple analytic spiral K-space algorithm. *Magn. Reson. Med.* **42**, 412–415 (1999).
47. Nestares, O. & Heeger, D.J. Robust multiresolution alignment of MRI brain volumes. *Magn. Reson. Med. [In Process Citation]* **43**, 705–715 (2000).
48. Teo, P.C., Sapiro, G. & Wandell, B.A. Creating connected representations of cortical gray matter for functional MRI visualization. *IEEE Trans. Med. Imaging* **16**, 852–863 (1997).
49. Wandell, B.A. Computational neuroimaging of human visual cortex. *Annu. Rev. Neurosci.* **22**, 145–173 (1999).
50. Engel, S., Zhang, X. & Wandell, B. Colour tuning in human visual cortex measured with functional magnetic resonance imaging. *Nature* **388**, 68–71 (1997).